ISSN 0717-3644
ISSN online 0718-221X

Maderas. Ciencia y tecnología 7(2): 87-98, 2005

MATHEMATICAL MODELLING AND EXPERIMENTAL INVESTIGATION OF DEHUMIDIFIER DRYING OF RADIATA PINE TIMBER♣

Z. F. Sun[1], C. G. Carrington[1], C. Davis[1], Q. Sun[1], S. Pang[2]

ABSTRACT

A dynamic kiln-wide wood drying model was developed previously to solve the integral form of the unsteady-state mass, momentum and energy balance equations in the air side. For the wood side, an empirical model, characteristic drying curve, for the internal moisture movement is used, which was obtained for low and medium temperature drying of *Pinus radiata*, with a medium velocity of 1.4-4.1 m s^{-1}. As part of the research programme to improve the design and control of dehumidifier wood drying kilns, the wood drying model has been assessed using the experimental data measured under drying conditions similar to those in dehumidifier kiln. It is noted that close agreement between the modelled results and the experimental data can be obtained for *Pinus radiata* drying processes with a medium air velocity (< 5 m s^{-1}). However, larger discrepancy between the modelled results and the measured data has been observed with a higher velocity (8 m s^{-1}). To solve this problem a new characteristic drying curve, based on a two-zone diffusion model, has been used in the kiln-wide wood drying model and more accurate results have been obtained.

Keywords: characteristic drying curve; dehumidifier drying, kiln stack, mathematical model, *Pinus radaiata*, sapwood timber

INTRODUCTION

Modelling of the kiln-wide drying processes is essential for improving the design and analysis of wood drying equipment. A dynamic wood drying model has been developed, which solves the mass, momentum and energy balance equations for both the air flow and wood boards in drying three types of stack: normal stack, aligned stack and staggered stack (Sun and Carrington, 1999a; Sun and Carrington, 1999b; Sun, Carrington and Bannister, 2000). For the airflow inside a stack, the model solves the integral form of the unsteady-state mass, momentum and energy balance equations. For the wood side, the characteristic drying curve method (Keey, 1992) is adopted for the description of the internal moisture transfer processes inside the wood boards.

Models for detailed internal moisture transfer and heat transfer within wood boards have been established by Stanish *et al.* (1986) and Perré (1996). However, it is difficult to use these models for modeling kiln-wide wood drying processes, since very large computational time and computer storage are required. On the basis of the moisture movement mechanisms, a characteristic drying curve correlation was used by Pang (1994) for high-temperature drying and was obtained by Sun *et al.* (1996) for low and medium temperature drying of *Pinus radiata* sapwood with a medium velocity of 1.4-4.1 m s^{-1}. These correlations relate the normalized drying rate to the conventional normalized

[1] Physics Department, University of Otago,PO Box 56, Dunedin, New Zealand.
[2] Department of Chemical and Process Engineering, University of Canterbury, Christchurch, New Zealand
Corresponding author: zhifa@physics.otago.ac.nz
Received: 21.06.2005. Accepted: 03.08.2005.

moisture content using the equilibrium moisture content, the critical moisture content and the normalized moisture content defined in terms of the fibre saturation point (FSP) and the critical moisture content. In particular, two constant parameters were used in the correlation, which were noted previously to be dependent on board geometry and wood structure properties (Sun *et al.,* 1996). However, the effect of drying conditions, such as air velocity, temperature, and humidity on the two parameters has not been considered. Consequently, the application of this characteristic drying curve may be restricted.

In this paper, the kiln-wide drying model and the characteristic drying curve have been further assessed by comparison of calculated results with the measured data obtained by Pang (1999) and by Davis (2001). In order to overcome the difficulty that the present drying curve relation is not accurate for cases where the air velocity is high, a new characteristic drying curve, based on the two-zone diffusion model developed by Davis (2001), has been established and tested.

WOOD DRYING MODEL

The dynamic model used in modelling kiln-wide wood drying processes has been described in detail in previous papers (Sun and Carrington, 1999a; Sun and Carrington, 1999b; Sun *et al.*, 2000). For simplicity, the air flow model is one-dimensional, but two parallel air streams for the central stack and side stack are used.

The characteristic drying curve method (Keey, 1992) was adopted for the description of the internal moisture transfer processes inside wood boards. When the surface of the moist-wood is no longer saturated with moisture, the characteristic drying-curve concept can be used to relate the unhindered drying rate from saturated surface to the diminished drying rate (Ashworth, 1977; Keey, 1992; Pang, 1994). Thus, from the Fick's first law of diffusion, the real drying rate can be written as

$$m_v^{(m)} = \frac{\omega_v^{(m)} m_a^{(m)}}{(1-\omega_v^{(m)})} + \frac{f k_\omega A_c (\omega_{v,sat}^{(m)} - \omega_v)}{(1-\omega_{v,sat}^{(m)})} \qquad (1)$$

where f is the normalized drying rate, which is defined as the ratio of the diminished drying rate to the unhindered drying rate and k_ω is the mass transfer coefficient, on the basis of the vapour mass fraction difference between the surface of wood boards and the bulk air stream.

An empirical characteristic drying curve relation for the internal moisture movement was proposed for drying of *Pinus radiata* sapwood (Sun *et al.,* 1996). For the constant rate period ($X \geq X_c$)

$$f = 1.0 \qquad (2)$$

For the falling rate period ($X < X_c$),

$$f = \Phi^{A - B\Phi_{fsp}} \qquad (3)$$

where

$$\Phi = \frac{X - X_e}{X_c - X_e} \qquad (4)$$

and

$$\Phi_{fsp} = \frac{X - X_{fsp}}{X_c - X_{fsp}} \qquad (5)$$

In the equations above, X_c is the critical moisture content; X_e is the equilibrium moisture content; X_{fsp} is the fibre saturation point. The two constant parameters, A and B, in Eq.(3) were noted previously to be dependent on board geometry and wood structure properties, of which fitted values were obtained for *Pinus radiata* sapwood at low and medium temperatures, with a velocity range of 1.4-4.1 m s^{-1} (Sun *et al.,* 1996).

In the wood drying model, the external mass-transfer and heat-transfer coefficients are evaluated by using empirical correlations. Due to the boundary layer separation, reattachment, and redevelopment of flow, measured mass and heat transfer data over blunt-edged flat plates show a common characteristic that the transfer rate is maximum at the point of reattachment and passes through a minimum at a point between the leading edge and the reattachment point (Sørensen, 1969; Kho, 1993). The correlations for mass and heat transfer j-factors over blunt boards have been established by Sun (2002) and used in the kiln-wide wood drying model, which are given by

$$j = \left(0.0288 - \alpha \, \mathrm{Re}_x^{-\beta}\right) \mathrm{Re}_x^{-\left(0.2-\gamma \, \mathrm{Re}_x^{-\beta}\right)} \tag{6}$$

where α, β, and γ are positive parameters. Using the mass transfer data over blunt boards in a board stack measured by Kho (1993), the fitted correlations for the parameters α, β, and γ are obtained as follows:

$$\alpha = 2.1513 \times 10^{-6} \, \mathrm{Re}_D^{1.1106} \, \mathrm{Re}_S^{0.6501} \tag{7}$$

$$\beta = 0.1542 \, \mathrm{Re}_D^{0.1410} \, \mathrm{Re}_S^{0.0437} \tag{8}$$

and

$$\gamma = 8.5197 \times 10^{-5} \, \mathrm{Re}_D^{1.1172} \, \mathrm{Re}_S^{0.5240} \tag{9}$$

where Re_D (=4400~22,000) and Re_S (=4400~10,300) are the Reynolds numbers based on the board thickness and the space size between two board layers. For the region from the leading edge to the minimum point, the conventional power law relation for a turbulent boundary layer is used, with $\alpha = 0$, $\beta = 0$, and $\gamma = 0$ in Eq.(6) (Sun, 2002).

COMPARISON OF MODELLED RESULTS WITH THE MEASURED DATA

Simulation runs have been carried out under the experimental conditions of the five experiments performed by Pang (1999) and the experiments conducted by Davis (2001). Here, only the simulation results of the five experimental runs of Pang are presented. The simulation results of the experimental runs of Davis are presented elsewhere (Davis, 2001), which are consistent with the results shown below.

The material for the five experimental runs of Pang was *Pinus radiata* sapwood and all the runs were conducted in a tunnel dryer, using varying air temperature, humidity and air velocity (Pang, 1999). The measured data of green moisture content and wood density for each run have been used in the calculation as initial conditions. The total drying time for each run is based on the experimental values. The measured stack-on air velocity, dry-bulb temperature, and wet-bulb temperature were used as the boundary conditions for the calculation.

Table 1 lists the measured parameters and operating conditions in the experiment. The number of control volumes used in each of the simulation runs is the same as the number of the boards in a board layer in the experimental stacks.

In Runs 1 and 2, the dimensions of the sample timber were 200×40×580 mm^3 with 10 boards in each layer of the four-layer stack. The stack-on dry-bulb/wet-bulb temperatures were 45/35°C and 71/60°C respectively in runs 1 and 2. The air velocity was 8 m s^{-1} and airflow was reversed every 12 hours in both run 1 and run 2. In Runs 3, 4, and 5, the dimension of the sample timber was 100×40×590 mm^3 with 23 boards in each layer of the four-layer stack. The stack-on dry-bulb/wet-bulb temperatures 71/60.7°C, 71/60.8°C, and 60/47°C were used in Runs 3, 4, and 5 respectively. The stack-on wet-bulb temperatures used in the model were slightly different from the target values given in Table 1. These have been adjusted to agree with the measured stack-on wet-bulb temperatures obtained by Pang (1999). There is no basis for making this adjustment for runs 1 and 2, since no measured values were provided for the stack-on wet-bulb temperatures in runs 1 and 2. The airflow velocity used was 3, 5, and 3 m s^{-1} for Runs 3, 4, and 5 respectively. In Run 3, the airflow was reversed every 12 hours.

TABLE 1. Measured parameters and operating conditions in drying experiments (Pang, 1999)

Parameters for measurements or control	Run 1	Run 2	Run 3	Run 4	Run 5
Measured drying time, hours	153.9	91.4	132.0	108.0	136.0
Initial average MC of boards, %	165.6	164.9	131.8	159.3	158.7
Final average MC of boards, %	14.0	12.0	14.2	12.0	11.3
Average wood basic density, kg/m^3	436.0	401.0	459.0	419.0	422.0
Number of boards in a layer of the stack	10	10	23	23	23
Number of layers of the stack	4	4	4	4	4
Total volume of timber in the kiln, m^3	0.1856	0.1856	0.2171	0.2171	0.2171
Total width of the stack, m	0.58	0.58	0.59	0.59	0.59
Total depth of the stack, m	2.0	2.0	2.3	2.3	2.3
Board thickness, mm	40	40	40	40	40
Fillet thickness, mm	20	20	20	20	20
Air velocity between boards, m s^{-1}	8	8	3	5	3
Air-flow reversal interval, hours	12	12	12	–	–
Dry-bulb/wet-bulb, °C	45/35	71/60	71/60	71/60	60/46

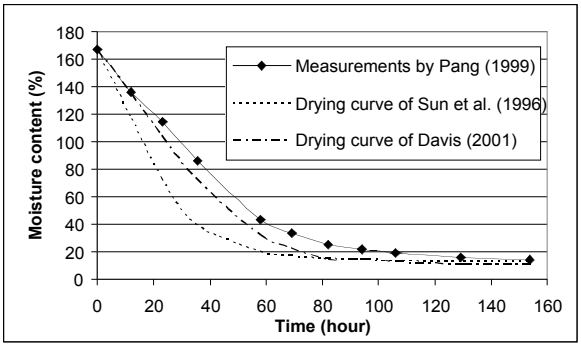

Fig. 1. Variation of the average moisture content in Run 1.

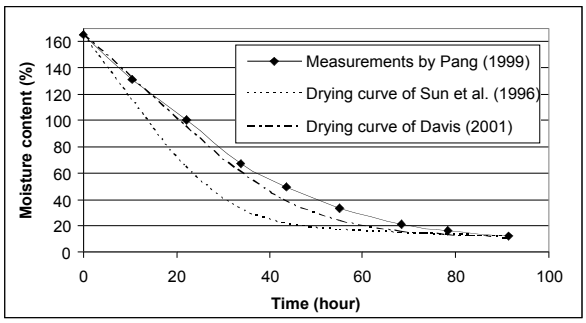

Fig 2. Variation of the average moisture content in Run 2.

Figures 1 and 2 show the modelled and measured average moisture content profiles. In these figures and Figures 3 to 7 below, the dashed lines represent the simulated results obtained using the characteristic drying curve of *Sun et al.* (1996) and the points denote the measured values of Pang (1999). The dot-dashed lines represent the results obtained using a separate characteristic drying curve based on the two-zone diffusion model developed by Davis (2001), which is described below. Referring just to the simulated drying curve of Sun *et al.* (1996), these figures indicate that there are large discrepancies between the modelled moisture contents and the measured moisture contents in the early period of the wood drying processes. The drying rate is overestimated by the model. One of the possible reasons for the calculation errors is that the characteristic drying curve used in the model was obtained based on the measured data obtained in a lower velocity range of 1.4-4 m s^{-1} (Sun *et al.*, 1996), which is much lower than the air velocity of 8 m s^{-1} in both Run 1 and Run 2. For a drying process with a high air velocity (>5 m s^{-1}), this drying curve may not be applicable.

Figures 3, 4, and 5 show the modelled and measured average moisture content profiles for Runs 3 to 5. It is seen that the discrepancies between the results obtained using the drying curve of Sun *et al.* (1996) and the measured values are much smaller than those shown in Figures 1 and 2 for Runs 1 and 2. It is noted that the airflow velocity, 3 m s^{-1}, in Runs 3 and 5 is in the velocity range of 1.4-4 m s^{-1}, at which the characteristic drying curve was obtained (Sun *et al.,* 1996). The air velocity, 5 m s^{-1}, in Run 4 is close to the velocity range. This suggests that the kiln-wide wood drying model and the characteristic drying curve of Sun *et al.* (1996) can only be used for modeling drying processes with an air velocity less than 5 m s^{-1}.

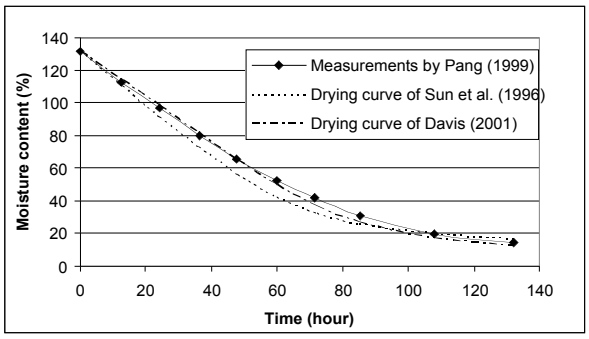

Fig. 3. Variation of the average moisture content in Run 3.

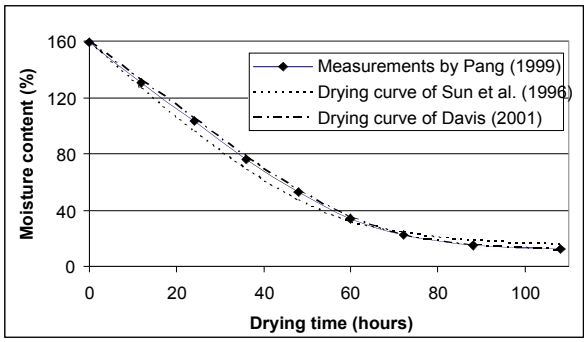

Fig. 4. Variation of the average moisture content in Run 4.

Figures 6 and 7 show the modelled and measured moisture content distributions along the stack in Run 3 and Run 4 respectively. In these figures, the dashed lines represent the results obtained using the characteristic drying curve of Sun *et al*. (1996) and the points denote the values measured by Pang (1999). These figures also indicate that the drying process of *Pinus radiata* sapwood with a lower velocity (< 5 m s^{-1}) can be described by the kiln-wide wood drying model and the characteristic drying curve expressed by Eqns.(2)-(5), with reasonable accuracy.

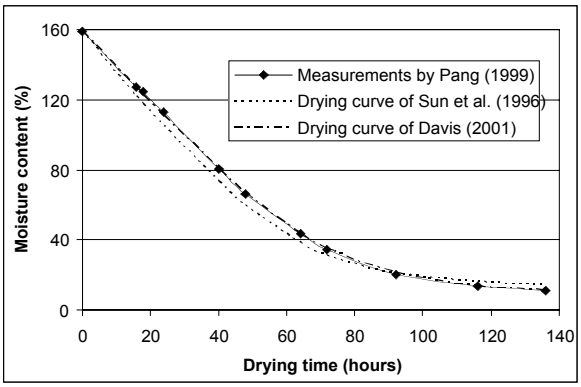

Fig. 5. Variation of the average moisture content in Run 5.

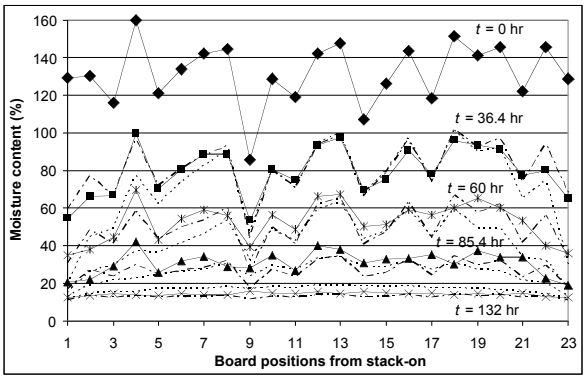

Fig. 6. Moisture content distribution along the stack in Run 3.

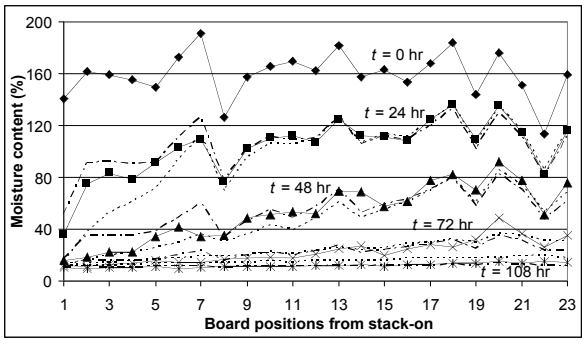

Fig 7. Moisture content distribution along the stack in Run 4.

It is seen from Figure 6 that due to the airflow reversal in Run 3, the moisture contents at the stack-on and stack-off positions of the stack are lower than that at the middle of the stack. Since the air

stream is not reversed in Run 4, Figure 7 shows that the moisture content at the stack-on is significantly lower than that at the stack-off.

The modelled and measured stack-off dry-bulb temperatures in Runs 4 and 5 are compared in Figure 8. The thinner solid lines represent the results obtained using the drying curve of Sun *et al.* (1996) and the points denote the values measured by Pang (1999). There are no measured stack-off dry-bulb temperatures for Runs 1 and 2 and no measured stack-off wet-bulb temperatures for comparison with the modelled results. Figure 8 indicates that the modelled stack-off dry-bulb temperatures are in reasonable agreement with the measured values. However, the calculated results of the stack-off temperature are generally larger than the measured values. The errors may be due to that we have neglected the heat losses between the air streams and the surroundings and the energy used for heating up the stack chamber in the calculation, which causes higher stack-off air temperatures compared with the measured values.

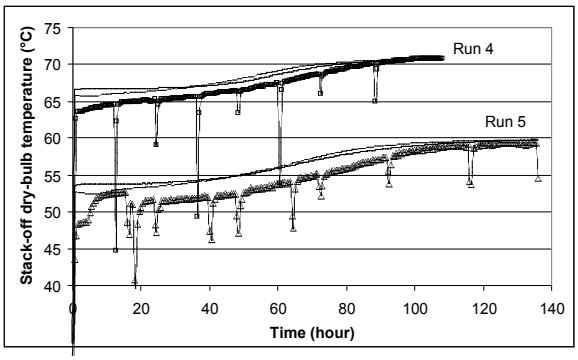

Fig. 8. Comparison of the measured and calculated stack-off dry-bulb temperatures in Runs 4 and 5.

CHARACTERISTIC DRYING CURVE BASED ON AN ISOTHERMAL DIFFUSION MODEL

As indicated by Figures 1 and 2, for drying processes of *Pinus radiata* with high airflow velocities, a more accurate drying curve is necessary.

An isothermal diffusion model has been developed by Davis (2001) for the analysis of *Pinus radiata* drying processes. Using an established desorption function, the model gives approximate analytic drying curve functions, which can be further converted to a characteristic drying curve.

The isothermal diffusion model assumes that the diffusion coefficient varies exponentially with moisture content below the fibre saturation point and is constant above the fibre saturation point, as follows (Davis, 2001),

$$D = D_0 \qquad X_{fsp} \le X \le X_0 \tag{10}$$

and

$$D = D_0 \exp\left[A\left(\frac{X - X_{fsp}}{X_0 - X_e} \right) \right] \quad X < X_{fsp} \tag{11}$$

where A is a constant parameter, D_0 is the local diffusion coefficient above FSP, and X_0 is the initial moisture content. The parameters A and D_0 are dependent on the properties of the material being dried and the operating conditions (Davis, 2001).

The boundary condition at the surfaces of wood boards utilises an apparent mass transfer coefficient, h_m', which accounts for the effect of an initial thin dry layer around the drying surfaces of the board (Pang, 1994). An empirical relationship was established between the apparent mass transfer coefficient, h_m', and the mass transfer coefficient of boundary layer theory, h_m, as given by (Davis, 2001),

$$\frac{h_m'}{h_m} \approx \frac{2.724 - 7.662\times10^{-3} T_\infty}{1 + 2.457\times10^{-7} \dfrac{h_m}{D_0}} \qquad (12)$$

where T_∞ is the temperature of the bulk airflow in Kelvin. This relation, along with the relations (10) and (11), allows straightforward prediction of drying curves for different types of *Pinus radiata* in different drying conditions and board dimensions. The resulting approximate drying curves are computationally inexpensive, and therefore suitable for kiln-wide models.

The conversion of the analytic drying curves to the characteristic drying curves is made by the transformation (Davis, 2001),

$$f = \frac{F}{\mathrm{Bi}'} \qquad (13)$$

where F is the dimensionless drying rate, and Bi[1] is the mass transfer Biot number which represents the ratio of internal mass transfer resistance to external mass transfer resistance.

TABLE 2. Reference parameters in the drying curve of Davis

Run	A	$D_0\times10^9$ ($m^2\ s^{-1}$)
1	0.001	2.63
2	0.001	2.63
3	0.001	1.70
4	0.001	2.50
5	0.001	1.70

The fitted values of A and D_0 used in modelling the experimental Runs 1-5 of Pang (1999) are listed in Table 2. Sensitivity analyses indicate that the kiln-wide wood drying model is much less sensitive to the parameter A than the parameter D_0.

The new characteristic drying curve, which is based on the isothermal diffusion model, has been incorporated into the kiln-wide wood drying model. The modeled average moisture content profiles for Runs 1-5 are shown in Figures 1 to 5 as the dot-dashed lines. The modelled moisture content distributions along the stacks for Runs 3 and 4 are shown in Figures 6 and 7 as the dot-dashed lines. The modelled dry-bulb temperatures for Runs 4 and 5 are shown in Figure 8 as the thicker solid lines.

All these figures show that the modelled results using the new characteristic drying curve are in close agreement with the measured data. In particular, the large discrepancies between the modelled results, obtained using the drying curve of Sun *et al.* (1996), and the measured data for Runs 1 and 2 with a high air velocity have been reduced significantly.

CONCLUSION

The kiln-wide wood drying model of Sun and Carrington (1999a, 199b) and their colleagues (Sun *et al.*, 2000) using the characteristic drying curve of Sun *et al.* (1996) have been assessed using the experimental data obtained by Pang (1999) under dehumidifier drying conditions with low to medium temperatures.

It has been found that at a medium velocity (< 5m s^{-1}), the kiln-wide wood drying model together with the characteristic drying curve can give reasonably accurate descriptions of kiln performances. However, at a high air velocity (8m s^{-1}), large discrepancies between the results obtained using the characteristic drying curve of Sun *et al.* (1996) and the measurements have been noticed.

To solve this problem, a new characteristic drying curve, based on an isothermal diffusion model developed by Davis (2001), has been established and incorporated into the kiln-wide wood drying model. This new characteristic drying curve considers evaporation from a surface below a thin layer saturated at some temperature between the wet- and dry-bulb temperatures (Pang, 1994) and takes account of the effect of an initial dry thin surface layer on mass transfer. The results obtained using the new characteristic drying curve are in close agreement with the measured data. In particular, the large discrepancies between the modelled results and measured data in the cases of high air velocities have been reduced significantly. This suggests that the new characteristic drying curve can be successfully used for a wider range of velocities up to 8 m s^{-1}.

NOTA

♣This paper was first presented at the 8th IUFRO International Wood Drying Conference, Brasov, Romania and up-dated for MADERAS: Ciencia y Tecnología journal.

REFERENCES

Ashworth, J. C. 1977. The Mathematical Simulation of Batch-Drying of Softwood Timber. Ph.D. Thesis, Department of Chemical Engineering, University of Canterbury, New Zealand.

Davis, C. 2001. Dehumidifier Drying of P. Radiata Boards. Ph.D. Thesis, Physics Department, Otago University, New Zealand.

Keey, R. B. 1992. *Drying of Loose and Particulate Materials*. Hemisphere Publishing Corporation, New York.

Kho, P. C. S. 1993. Mass Transfer from In-Line Slabs. Ph.D. Thesis, Department of Chemical and Process Engineering, University of Canterbury, New Zealand.

Pang, S. 1994. High-Temperature Drying of *Pinus radiata* Boards in a Batch Kiln. PhD Thesis. University of Canterbury, New Zealand.

Pang, S. 1999.
Drying of Radiata Pine Lumber under Dehumidifier Conditions: Experiments and Model Simulation. Research Report, Forest Research, Rotorua, New Zealand.

Perré, P. 1996. The numerical modelling of physical and mechanical phenomena involved in wood drying: an excellent tool for assisting with the study of new processes. pp11-38. In: Cloutier, A., Fortin, Y. and Gosselin, R. (Ed.). Proceedings of the 5th IUFRO International Wood Drying Conference. August 13-17. Quebec City, Canada.

Sørensen, A. 1969. Mass transfer coefficients on truncated slabs. *Chemical Engineering Science* 24: 1445-1460.

Stanish, M. A.; Schajer, G. S.; Kayihan, F. 1986. A mathematical model of drying for hygroscopic porous Media. *AIChE Journal* 32 (8): 1301-1311.

Sun, Z. F.; Carrington, C. G.; McKenzie, C.; Bannister, P.; Bansal B. 1996. Determination and application of characteristic drying-rate curves in dehumidifier wood drying. pp495-503. In: Cloutier, A., Fortin, Y. and Gosselin, R. (Ed.). Proceedings of the 5th IUFRO International Wood Drying Conference. August 13-17. Quebec City, Canada.

Sun, Z. F.; Carrington, C. G. 1999a. Dynamic modelling of a dehumidifier wood drying kiln. *Drying Technology* 17 (4 & 5): 711-729.

Sun, Z. F.; Carrington, C. G. 1999b. Effect of Stack Configuration on Wood Drying Processes. pp89-98. In: Vermaas, H. and Steinmann, D. (Ed.). Proceedings of the 6th IUFRO International Wood Drying Conference. January 25-28. Stellenbosch, South Africa.

Sun, Z. F.; Carrington, C. G.; Bannister, P. 2000. Dynamic modelling of the wood stack in a wood drying kiln. *Trans Ichem E* 78, Part A: 107-117.

Sun, Z. F. 2002. Correlations for mass transfer coefficients over blunt boards based on modified boundary layer theories. *Chemical Engineering Science* 57 (11): 2029-2033.

NOTATION

A_c contact area between air and wood board (m^2)
Bi' mass transfer Biot number
D wood board thickness (m)
D_0 local diffusion coefficient ($m^2\ s^{-1}$)
f friction factor or normalised drying rate
F dimensionless drying rate
j Chilton-Colburn *j*-factor for mass and heat transfer
k_{ω} mass transfer coefficient (kg $m^{-2}\ s^{-1}$)
h_m mass transfer coefficient (kg $m^{-2}\ s^{-1}$)
$m_a^{(m)}$ mass transfer rate of dry air (kg s^{-1})
$m_v^{(m)}$ mass transfer rate of moisture (kg s^{-1})

Re_D Reynolds number ($=u_\omega D/\nu$)
Re_S Reynolds number ($=u_\omega S/\nu$)
Re_x local Reynolds number ($=u_\omega x/\nu$)
S space between board layers (m)
T_∞ temperature of the bulk air flow (K)
u_∞ velocity of the bulk air flow (m s^{-1})
x coordinate (m)\\\
X moisture content (kg kg^{-1})
X_0 initial moisture content (kg kg^{-1})

Greek symbols

Φ normalized moisture content
ν kinematic viscosity (m^2 s^{-1})
$\underline{\omega}$ mass fraction

Subscripts

a air
c critical point
e equilibrium point
fsp fibre saturation point
sat at saturation
v vapour

Superscripts

(m) quantity crossing board surface